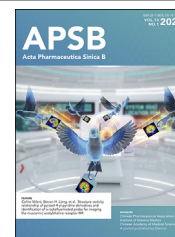




Chinese Pharmaceutical Association  
Institute of Materia Medica, Chinese Academy of Medical Sciences

Acta Pharmaceutica Sinica B

[www.elsevier.com/locate/apsb](http://www.elsevier.com/locate/apsb)  
[www.sciencedirect.com](http://www.sciencedirect.com)



ORIGINAL ARTICLE

# *Chlorella* sp.-ameliorated undesirable microenvironment promotes diabetic wound healing



Hangyi Wu<sup>a</sup>, Pei Yang<sup>a</sup>, Aiqin Li<sup>a</sup>, Xin Jin<sup>a,b</sup>, Zhenhai Zhang<sup>c,d,\*</sup>,  
HuiXia Lv<sup>a,\*</sup>

<sup>a</sup>Department of Pharmaceutics, China Pharmaceutical University, Nanjing 211198, China

<sup>b</sup>The Affiliated Suqian First People's Hospital of Nanjing Medical University, Suqian 223800, China

<sup>c</sup>Jiangsu Province Academy of Traditional Chinese Medicine, Nanjing 210023, China

<sup>d</sup>Affiliated Hospital of Integrated Traditional Chinese and Western Medicine, Nanjing University of Chinese Medicine, Nanjing 210028, China

Received 8 February 2022; received in revised form 29 April 2022; accepted 12 May 2022

## KEY WORDS

*Chlorella* sp.;  
Diabetic wound healing;  
Oxygen production;  
Glucose consumption;  
ROS depletion;  
Nutrition supplement;  
Anti-inflammation

**Abstract** Chronic diabetic wound remains a critical challenge suffering from the complicated negative microenvironments, such as high-glucose, excessive reactive oxygen species (ROS), hypoxia and malnutrition. Unfortunately, few strategies have been developed to ameliorate the multiple microenvironments simultaneously. In this study, *Chlorella* sp. (*Chlorella*) hydrogels were prepared against diabetic wounds. *In vitro* experiments demonstrated that living *Chlorella* could produce dissolved oxygen by photosynthesis, actively consume glucose and deplete ROS with the inherent antioxidants, during the daytime. At night, *Chlorella* was inactivated *in situ* by chlorine dioxide with human-body harmless concentration to utilize its abundant contents. It was verified *in vitro* that the inactivated-*Chlorella* could supply nutrition, relieve inflammation and terminate the oxygen-consumption of *Chlorella*-respiration. The advantages of living *Chlorella* and its contents were integrated ingeniously. The abovementioned functions were proven to accelerate cell proliferation, migration and angiogenesis *in vitro*. Then, streptozotocin-induced diabetic mice were employed for further validation. The *in vivo* outcomes confirmed that *Chlorella* could ameliorate the undesirable microenvironments, including hypoxia, high-glucose, excessive-ROS and chronic inflammation, thereby synergistically promoting tissue regeneration. Given the results above, *Chlorella* is considered as a tailor-made therapeutic strategy for diabetic wound healing.

\*Corresponding authors. Tel./Fax.: +86 13912965842; +86 18913823932.

E-mail addresses: [david23932@163.com](mailto:david23932@163.com) (Zhenhai Zhang), [Lvhuixia@163.com](mailto:Lvhuixia@163.com) (HuiXia Lv).

Peer review under the responsibility of Chinese Pharmaceutical Association and Institute of Materia Medica, Chinese Academy of Medical Sciences.

<https://doi.org/10.1016/j.apsb.2022.06.012>

2211-3835 © 2023 Chinese Pharmaceutical Association and Institute of Materia Medica, Chinese Academy of Medical Sciences. Production and hosting by Elsevier B.V. This is an open access article under the CC BY-NC-ND license (<http://creativecommons.org/licenses/by-nc-nd/4.0/>).

## 1. Introduction

Diabetes is a complex metabolic disease that affects millions of people globally. Roughly, 25% of the patients face diabetic ulcers which may cause amputation and even death<sup>1</sup>. Diabetic ulcer is a non-healing chronic wound with a high recurrence rate, ascribing its complex ulcer microenvironments which are characterized as high-glucose, excessive reactive oxygen species (ROS), severe hypoxia and malnutrition<sup>2–4</sup>, etc. Specifically, high-level blood glucose leads to the accumulation of advanced glycation end products (AGEs). AGEs can aggravate oxidative stress, reduce the phagocytic capacity of macrophages<sup>5</sup>, increase inflammatory cytokines secretion<sup>6,7</sup> and recruit more neutrophils and macrophages in the wound<sup>8</sup>. Then, the respiratory burst caused by macrophages and neutrophils further exacerbates ROS production, resulting in chronic inflammation<sup>9,10</sup>. Meanwhile, oxygen and nutrition will be consumed by inflammatory cells and blocked by ischemia, leading to a deterioration of the hypoxia and malnutrition<sup>11,12</sup>. The above-mentioned factors form a vicious circle and restrict the proliferation and migration of cells, the generation of extracellular matrix and angiogenesis, thereby limiting wound healing<sup>13–15</sup>. Existing treatments for diabetic wounds, such as hyperbaric oxygen therapy, cell-based therapy and drug combination therapy, have inconsistent outcomes and some of them are associated with undesirable side effects<sup>16</sup>. Furthermore, most of the therapeutics just act on one or two specific factors. However, the diabetic wound microenvironments are interconnected, which may limit the therapeutic efficacy. Thus, strategies that can simultaneously ameliorate the multiple negative tissue microenvironments of diabetic wounds via facile procedure are more attractive.

*Chlorella* sp. (*Chlorella*) is one of the most widely cultured microalgae species due to its rapid proliferation. *Chlorella* possesses abundant nutrition such as proteins, lipids, nucleic acid and vitamins, and has been named as “green healthy food” by the Food and Agriculture Organization of the United Nations<sup>17,18</sup>. *Chlorella* can continuously produce oxygen by photosynthesis, recognized as the origin of oxygen in the earth<sup>19–21</sup>. In recent years, living alga (*Synechococcus elongates*) has been proven to ameliorate the hypoxia in diabetic wounds, which gained superior oxygen transfer efficacy compared with the oxygen-based treatments commonly used<sup>22</sup>. However, in addition to the well-known photosynthesis, other wound healing-friendly functions of living microalgae are still unrevealed. Nitrogen and phosphorus can be solidified by algae, as well as glucose<sup>23</sup>. This seemed to be a benefit tailored to the high-glucose microenvironment of diabetic wound tissue. Given the rapid proliferation and the excellent metabolic activity, *Chlorella* might be a sharp weapon for glucose consumption. Furthermore, *Chlorella* could also promote tissue regeneration by depleting ROS with the high-content internal antioxidants, such as lutein and carotene<sup>24</sup>. Unfortunately, living algae are often accompanied by bacteria, which may elicit immune responses and aggravate oxidative stress, thereby limiting their applications in wounds. In addition to the abovementioned advantages, the

contents of *Chlorella* could also be as desiderate nutrients for the ischemic tissue<sup>25</sup> and play an anti-inflammatory role<sup>26,27</sup>. Hence, *Chlorella* might be a potential strategy for regulating the multiple negative microenvironments.

In this study, axenic *Chlorella* was fixed in hydrogels against chronic diabetic wounds. The microenvironment regulation and tissue regeneration by *Chlorella* hydrogels were assessed *in vitro* and *in vivo*. Living *Chlorella* was proved to reverse serious hypoxia, consume high-level glucose as well as deplete excessive ROS during the daytime, while the *Chlorella* was inactivated at night to get rid of the side effect of *Chlorella*-respiration and enjoy the additional benefits of nutrition supplement and inflammation relief by the released contents (Schematic diagram). The results suggested that *Chlorella* could ameliorate the negative microenvironments of wound tissue and promote diabetic wound healing.

## 2. Materials and methods

### 2.1. Materials

Hyaluronic acid (HA) (900–1200 kDa) was a generous gift from BLOOMAGE BIOTECHNOLOGY Co., Ltd. (Beijing, China). *Chlorella* (FACHB-5) and Blue-Green medium (BG-11) was purchased from Freshwater Algae Culture Collection at the Institute of Hydrobiology (Wuhan, China). 4',6-Diamidino-2-phenylindole (DAPI), kanamycin and 2',7'-dichlorodihydrofluorescein diacetate (DCFH-DA) were obtained from Aladdin Co., Ltd. (Shanghai, China). Kits were purchased from Solarbio Life Sciences (Beijing, China). All other chemicals and reagents were obtained from Sinopharm Chemical Reagent Co., Ltd. (Nanjing, China).

### 2.2. Cell lines and animals

Human umbilical vein endothelial cells (HUVECs), human immortalized keratinocytes (HaCaTs), mouse skin fibroblasts (L-929) and RAW 264.7 macrophages were obtained from KeyGEN Biotech Co., Ltd. (Nanjing, China). HUVECs were incubated in ECM medium (Sciencell, CA, USA) supplemented with 5% (*v/v*) fetal bovine serum (FBS), 1% (*v/v*) penicillin–streptomycin (P/S) and 1% (*v/v*) endothelial cell growth supplement. HaCaTs, L-929 and RAW 264.7 macrophages were cultured in high-glucose Dulbecco's modified Eagle's medium (DMEM, Gibco, Thermo Fisher Scientific, MA, USA) supplemented with 10% fetal bovine serum FBS (*v/v*) and 1% (*v/v*) P/S in the incubator (37 °C, 5% CO<sub>2</sub>) (Thermo Fisher Scientific, MA, USA).

BALB/c mice (male, about 25 g in weight) obtained from Qing Longshan Animal Co., Ltd. (Nanjing, China) were fed at 25 °C and 55% humidity under natural light/dark cycles. All experimental procedures were executed according to the protocols approved by China Pharmaceutical University Animal Care and Use Committee.

### 2.3. Axenic culture establishment and assessment of *Chlorella*

#### 2.3.1. Axenic culture establishment

The *Chlorella* axenic culture was established by antibiotic treatments. In brief, the *Chlorella* solution was centrifuged (4000 rpm, 3 min, D3024R, DLAB, Beijing, China), and the supernatant was discarded. Then, the *Chlorella* precipitation was streaked on agar plates containing 80 mg/L kanamycin with transfer ring. After colonies formation, the individual *Chlorella* colonies were selected under a stereomicroscope (M205A, Leica, Germany) and streaked again. The cycle was repeated three times. Finally, the *Chlorella* was added to the sterile BG-11 medium and cultured with cell culture flasks in the biological safety cabinet (Thermo Fisher Scientific, MA, USA) (25 °C, 2500–3000 lx, 12 h:12 h light/dark cycle).

#### 2.3.2. Axenic culture assessment

To verify the axenic culture, the *Chlorella* precipitation was spread on antibiotic-free sterile BG-11 agar plates. After the colonies formation, the *Chlorella* was photographed by an inverted fluorescence microscope (IX53, Nikon, Japan).

The *Chlorella* was also verified with antibiotic-free sterile beef extract peptone agar plates. The *Chlorella* solution was sprayed on the beef extract peptone agar plates, and the photographs of colonies were captured after 24 h incubation.

The cytotoxicity of *Chlorella* was determined with Transwell (12-well, 0.4- $\mu$ m pore-size). In brief, the cells (L-929, HaCaT and HUVEC) were seeded in the lower chamber. After attachment, *Chlorella* solution ( $1 \times 10^9$  cell/mL) was added to the upper chamber. After 24 h incubation, the cell viability was measured by Cell Counting Kit-8 (CCK-8) assay.

### 2.4. Preparation and characterization of *Chlorella* hydrogel

#### 2.4.1. Preparation of *Chlorella* hydrogel

The *Chlorella* was centrifuged (4000 rpm, 3 min, DLAB), and the supernatant was discarded. The *Chlorella* precipitation was washed three times and re-suspended with BG-11 medium. The concentrations of re-suspended *Chlorella* were quantitated (*Chlorella* was counted with a microscope (Nikon)) to  $1 \times 10^6$ ,  $1 \times 10^7$ ,  $1 \times 10^8$  and  $1 \times 10^9$  cell/mL, respectively. Then, 2% HA *w/v* was added into the *Chlorella* solution and stirred to form the *Chlorella* hydrogels. The *Chlorella* hydrogels were named as CH6, CH7, CH8 and CH9, respectively.

#### 2.4.2. Characterization of *Chlorella* hydrogel

The hydrogels were photographed and tested by a scanning electron microscope (SEM, SU8010, Hitachi, Japan).

The cytotoxicity of *Chlorella* hydrogels was determined with Transwell (12-well, 0.4- $\mu$ m pore size). In brief, the cells (L-929, HaCaT and HUVEC) were seeded in the lower chamber. After attachment, *Chlorella* hydrogels were added to the upper chamber. After 24 h incubation (dark), the cell viability was measured by CCK-8 assay.

The storage stability of *Chlorella* hydrogels was detected. In brief, the *Chlorella* hydrogels were packed in penicillin vials and stored for 30 days, 4 °C, dark. The photographs of hydrogels were captured. Then, a 10-fold BG-11 medium (*v/v*) was added to the hydrogels for dilution, and the diluted solution was vortexed and centrifuged (4000 rpm, 3 min, DLAB). The proliferation of *Chlorella* (precipitation) was measured by CCK-8 assay. The

concentrations of  $\text{NO}_3^-$  remained in the hydrogels (supernatant) were determined by the NO kit (Nitrate reductase method).

### 2.5. *In vitro* oxygen production

#### 2.5.1. Oxygen production

Franz diffusion cells were employed to measure the oxygen production by *Chlorella*. The medium was deoxygenated before detection. In brief, a polytetrafluoroethylene membrane (0.22- $\mu$ m pore size) was fixed between the chambers. *Chlorella* hydrogel (1 mL) was added into the donor chamber, while phosphate-buffered saline (PBS) was injected into the receptor chamber (6.5 mL). The donor chamber was covered by an airtight transparent polyurethane film. *Chlorella* hydrogels were continuously exposed to daily used LED light with 800 lx (simulating the average illuminance during the daytime) or shaded with tinfoil (simulating the nighttime). At pre-determined time points (0.5, 1, 2, 4 and 8 h), PBS (0.5 mL) was taken out with a sampler and the oxygen level was detected by an oxygen electrode (AR8010, Smart Sensor, Hong Kang, China). After measurement, the deoxygenated PBS (0.5 mL) was supplemented into the receptor chamber. To further determine the transdermal delivery efficiency of oxygen, mice skin excised from the back was employed to substitute the polytetrafluoroethylene membranes. The stratum corneum of the skin was removed by tape.

#### 2.5.2. Breathing pattern inversion

The breathing pattern inversion ability of *Chlorella* hydrogels was reflected by adenosine triphosphate (ATP) level and lactic acid (LA) content. In brief, L-929 cells ( $1 \times 10^5$  cell/well) were plated into the lower chamber of the Transwell (12-well, 0.4- $\mu$ m pore size). After attachment, the Transwell was placed in hypoxia culture condition and balanced for 6 h. Then, the hydrogels were added to the upper chambers (800 lx). After 6 h incubation, L-929 cells were trypsinized, collected and crushed in sequence. The ATP level in the cells was detected by an ATP content kit, and LA content in the supernatant was tested by an LA content kit.

#### 2.5.3. Intracellular ROS test

The Transwell was designed as Section 2.5.2. After 12 h incubation, the cells were washed in triplicate using PBS and incubated with DCFH-DA (10  $\mu$ mol/L) for 20 min. After removing the free fluorescent dyes, the intracellular ROS level was measured by a confocal laser scanning microscope (CLSM, FV3000, Olympus, Japan).

### 2.6. *In vitro* glucose consumption

*Chlorella* was cultured in the BG-11 medium with 33 mmol/L glucose, stimulating the high-glucose condition. After 12 h incubation, the *Chlorella* was centrifuged (4000 rpm, 3 min) and the concentration of glucose in the supernatant was detected by the glucose kit. Three kinds of light intensities (dark; 10,000 lx, 1 h:11 h light/dark; 800 lx, continuous illumination) were involved to investigate the influence of illumination on glucose consumption.

The glucose fixation by *Chlorella* was also detected. After centrifuging (4000 rpm, 3 min), the *Chlorella* in the deposit was re-suspended and sacrificed (80 °C water bath for 1 h and ultrasound for 1 h, 40 kHz, 50% power ratio). The glucose inside the *Chlorella* was measured by the glucose kit.

The inherent glucose concentration of Chlorella was also detected. In brief, fresh Chlorella solution was centrifuged (4000 rpm, 3 min) and sacrificed (80 °C water bath for 1 h and ultrasound for 1 h, 40 kHz, 50% power ratio). Then, the glucose inside the Chlorella was measured by the glucose kit.

Transwell (12-well, 0.4- $\mu$ m pore size) was employed to test the consumption of glucose mimicking the condition in wound tissue. Chlorella hydrogel was added to the upper chamber, and PBS with 33 mmol/L glucose was applied in the lower chamber. After 12 h incubation, the concentration of glucose in the lower chamber was determined.

## 2.7. *In vitro* ROS depletion

To analyze the depletion efficiency of H<sub>2</sub>O<sub>2</sub>, Chlorella and inactivated-Chlorella (explained in 2.8) were added into the BG-11 medium with 16.3 mmol/L H<sub>2</sub>O<sub>2</sub> for 20 min (according to the kit) (dark; 800 lx; 10,000 lx), respectively. After incubation, the medium was centrifuged (4000 rpm, 3 min) and the supernatant was collected. The concentration of H<sub>2</sub>O<sub>2</sub> in the supernatant was detected by the H<sub>2</sub>O<sub>2</sub> kit.

The  $\cdot\text{OH}^-$  and  $\cdot\text{O}_2^-$  scavenging capacities were also investigated, respectively. In brief, the Chlorella solution was incubated with the standard solution provided by the kit. At the pre-determined time points, the  $\cdot\text{OH}^-$  (1 min) and  $\cdot\text{O}_2^-$  (40 min) scavenging capacities of Chlorella were tested as described by the manufacturer, respectively.

The depletion of ROS was also measured with Transwell (12-well, 0.4- $\mu$ m pore size). In brief, Chlorella hydrogels and inactivated-Chlorella hydrogels were added to the upper chamber of the Transwell, respectively. The lower chamber was filled up with 16.3 mmol/L H<sub>2</sub>O<sub>2</sub> and  $\cdot\text{OH}^-/\cdot\text{O}_2^-$  substrate (37 °C, dark), respectively. At the predetermined time point, the solution in the lower chamber was collected and measured by kits.

## 2.8. Chlorella inactivation

### 2.8.1. Chlorella inactivation by chlorine dioxide

The efficiency of Chlorella inactivation by chlorine dioxide was exemplified with CH8 (CH8 was the best among the selected hydrogels in the pre-experiment of *in vivo* diabetic wound healing). CH8 (350  $\mu$ L) was added to the upper chamber of the Transwell (12-well, 0.4- $\mu$ m pore size), and the lower chamber was filled up with PBS. Then, chlorine dioxide (1, 2, 5, 10 and 20 ppm, 50  $\mu$ L) was dripped onto the hydrogels to inactivate the Chlorella. At the pre-determined time points (0, 5, 10 and 15 min, and 12 h), the inactivated-Chlorella hydrogels were photographed. At 15 min and 12 h time points, the inactivation process was terminated by sodium thiosulfate<sup>28</sup>, and the inactivation efficiency was detected by CCK-8 assay.

The toxicity of Chlorella inactivation was also determined. The concentration of chlorine dioxide in the lower chamber (at 5, 15 and 30 min, 1 and 2 h time points after chlorine dioxide dripped) was measured by a chlorine dioxide analyzer (SJG-791, INESA Scientific Instrument, Shanghai, China). To verify the cytotoxicity of remaining chlorine dioxide, L-929 cells ( $1 \times 10^5$  cell/well) were seeded in 12-well plates. After attachment, DMEM containing the chlorine dioxide with the highest remaining concentration in the lower chamber during the inactivation was added. After 24 h incubation, the cytotoxicity was measured by CCK-8 assay.

Chlorella hydrogels (CH6, CH7, CH8 and CH9) with suitable concentrations of chlorine dioxide were named as CH6-C, CH7-C, CH8-C and CH9-C, respectively.

### 2.8.2. Chlorella contents release

Inactivated-Chlorella hydrogels were added to the upper chamber of the Transwell (12-well, 0.4- $\mu$ m pore size), and PBS was added to the lower chamber. Then, the plate was put into a shaker (60 rpm, ZD85, Jingda instrument manufacturing, Changzhou, China). At the pre-determined time points (1, 2, 4, 8 and 12 h), the PBS in the lower chamber was collected. The released Chlorella contents (carbohydrate, protein and nucleic acid) were detected by kits and OD260, respectively.

## 2.9. *In vitro* anti-inflammation

### 2.9.1. Macrophages cytokines secretion

RAW 264.7 cells ( $5 \times 10^4$  cell/well) were plated into the lower chamber of the Transwell (12-well, 0.4- $\mu$ m pore size) and stimulated with 2  $\mu$ g/mL LPS after attachment. Then, the hydrogels with Chlorella and inactivated-Chlorella were added to the upper chamber, respectively. After 24 h incubation, the medium in the lower chamber was collected, and the levels of IL-6, TNF- $\alpha$  and NO were assessed by the kits according to the manufacturer's instructions.

### 2.9.2. Macrophage transwell migration assay

HaCaT cells ( $5 \times 10^4$  cell/well) were seeded in the lower chamber of the Transwell and stimulated with 10  $\mu$ g/mL LPS to form the inflammatory cells<sup>29</sup>. Then, the hydrogels with Chlorella and inactivated-Chlorella were added to the upper chamber (12-well, 0.4- $\mu$ m pore size), respectively. After 24 h incubation, the upper chamber was substituted by the one (12-well, 8- $\mu$ m pore size) with attached RAW 264.7 cells (initial concentration,  $1 \times 10^4$  cell/well). After 24 h, the cells remaining on the upper surface of the filter were removed by a cotton swab. The migrated cells binding on the bottom side were stained with crystal violet solution. After washing in triplicate, the cells were photographed with an inverted fluorescence microscope (Nikon).

## 2.10. *In vitro* tissue regeneration

L-929s, HaCaTs and HUVECs were employed to evaluate *in vitro* tissue regeneration. All the cell assays were performed with Transwell. The specific incubation conditions were explained in the part of "Results and discussions". The results were quantified with ImageJ software (National Institutes of Health).

### 2.10.1. Proliferation assay

L-929 cells ( $1 \times 10^5$  cell/well) were seeded in the lower chamber (12-well, 0.4- $\mu$ m pore size) and incubated overnight for attachment. The Chlorella hydrogel was added to the upper chamber. After 24 h, cells were rinsed with PBS in triplicate and then stained with Calcein-AM. After the free fluorescent was removed, cells were observed under CLSM (Olympus).

### 2.10.2. *In vitro* scratch assay

HaCaT cells ( $2 \times 10^5$  cell/well) were plated in the lower chamber (12-well, 0.4- $\mu$ m pore size), forming a confluent monolayer. After starvation for 24 h, the cell monolayer was scratched by a 200  $\mu$ L pipette tip. Then, Chlorella hydrogel was added to the upper

chamber. After incubation for 24 h, the cells were photographed with an inverted fluorescence microscope (Nikon).

### 2.10.3. Transwell migration assay

HUVEC cells were plated in the upper chamber (12-well, 8- $\mu$ m pore size), while Chlorella hydrogel was added into the lower chamber within a dialysis bag (300 kDa). After 24 h, cells remaining on the upper surface of the Transwell membrane were removed by a cotton swab. The migrated cells binding on the bottom side were stained with crystal violet solution. After being washed in triplicate, the cells were photographed with an inverted fluorescence microscope (Nikon).

### 2.11. In vivo diabetic wound healing

The diabetic mice were established as commonly reported. In brief, streptozotocin (55 mg/kg) citrate buffer solution was intraperitoneally injected for five consecutive days after 4 weeks of high-fat and high-sugar feed. Mice with plasma glucose levels  $\geq 16.7$  mmol/L were considered diabetic. After 2 weeks, the mice were anesthetized by intraperitoneally injected with chloral hydrate and the backs were shaved. Then, a rounded full-thickness cutaneous wound with a diameter of 8 mm was performed by biopsy punch, and a silicone insert was stitched around the wound with non-absorbable sutures. The mice were randomly divided into eight groups: non-diabetes control (control), diabetes control (DM), CH6, CH7, CH8, CH9 (front six groups: 800 lx, 12 h:12 h light/dark cycle), CH8-D (CH8 without illuminate, D means dark) and CH8-C (chlorine dioxide was secondary delivery after 12 h light, C means chlorine dioxide). The control group and DM group were given HA hydrogels. All the hydrogels were renewed daily.

The wounds were photographed on Days 0, 3, 7 and 10 and evaluated by ImageJ software (National Institutes of Health). The scabs were removed for accurate quantification. Three mice in each group were randomly euthanized on Days 3, 7 and 10. Wound tissues were collected and fixed in 4% paraformaldehyde. Then, the samples were embedded in paraffin and sectioned (5  $\mu$ m). Immunofluorescence analysis (IL-6, Ki67, VEGF and CD31 immunostaining on Day 3 and Day 7, respectively) and histological analysis (H&E staining and Masson staining on Day 10) were performed according to the manufacturer's instruction. Granulation tissue gap, epithelial thickness, hair follicle density and re-epithelialization<sup>30</sup> were calculated according to H&E staining. Collagen deposition was evaluated with Masson staining.

### 2.12. In vivo wound microenvironment regulation

To verify the potential of Chlorella hydrogels for diabetic wound microenvironment regulation, the wound tissue was homogenized. ATP, LA, glucose and H<sub>2</sub>O<sub>2</sub> levels were determined by the corresponding kits on Days 3 and 7, respectively. The pH in the exudate of the wound was measured by a glass surface pH electrode (E-201-P, INESA Scientific Instrument, Shanghai, China) on Days 3 and 7.

### 2.13. Statistical analysis

Statistically differences between groups were determined by *t*-test. *P* values less than 0.05 were considered significant. All the data were analyzed and expressed as the mean  $\pm$  standard deviation (SD).

## 3. Results and discussions

### 3.1. Chlorella axenic culture

Chlorella and its productions are commonly used after inactivation by oral administration<sup>31</sup>. During the cultivation, Chlorella is often accompanied by bacteria, while the side effects of the Chlorella-associated bacteria are masked by the inactivation processing and the protection of the gastrointestinal tract<sup>31,32</sup>. In this study, Chlorella was fixed in the hydrogel and utilized in wound tissue. In the pre-experiment, treatment with non-axenic Chlorella showed increased inflammation and poor wound healing, which might be due to the lacked biological barriers in wound tissue. Herein, Chlorella axenic culture was applied.

In our study, Chlorella was purified by antibiotic treatment (Supporting Information Fig. S1). The obtained axenic Chlorella grew vigorously on the sterile BG-11 agar plate, while the proliferation of the non-axenic one was inhibited and even suspended over time (Fig. 1A). In the BG-11 medium, a small number of bacteria could be masked due to the adsorption and competitive inhibition of Chlorella. Hence, the axenic validation was further performed on the beef extract peptone agar plate. As shown in Fig. 1B, there were no bacterial colonies on the plate with axenic Chlorella, while bacterial colonies formed in the untreated group. Given the results above, the Chlorella was considered axenic.

The biological functions of Chlorella are closely related to the biomass. However, the non-axenic Chlorella often aggregates with bacteria, influencing the dispersibility and the count accuracy. This disadvantage could be improved by axenic culture. After 12 h standing, the sedimentation rate of axenic Chlorella was significantly lower than that of the untreated group, and there were no Chlorella-bacteria aggregates after axenic culture (Fig. 1C). The biocompatibility of Chlorella was also evaluated. As shown in Fig. 1D, axenic Chlorella was none toxicity to L-929, HaCaT and HUVEC cells.

Chlorella with concentrations of  $1 \times 10^6$ ,  $1 \times 10^7$ ,  $1 \times 10^8$  and  $1 \times 10^9$  cell/mL was exemplified in the following study.

### 3.2. Characterization of Chlorella hydrogel

Hydrogels are widely used for diabetic wound healing. They can maintain the humidity of the wound and remove exudate<sup>33</sup>. In this study, 2% HA with BG-11 medium was employed to fix Chlorella. Axenic Chlorella with gradient concentrations was uniformly dispersed in the hydrogels (Fig. 1E and F). The Chlorella hydrogels were proven to be non-toxic (Supporting Information Fig. S2). After 30-days of storage (4  $^{\circ}$ C, dark), all the hydrogels showed no delamination and aggregation (Fig. 1F), satisfying the storage stability for preclinical studies.

To avoid the unstable treatment efficacy caused by the variety of Chlorella biomass, the proliferation of Chlorella under the treatment conditions was confirmed. The results demonstrated that Chlorella with concentrations of  $1 \times 10^6$  and  $1 \times 10^7$  cell/mL proliferated at 22.4%, 21.7% in the BG-11 medium and 13.4%, 16.0% in the hydrogels for 24 h, respectively (Fig. 1G). Compared with the selected magnitude-concentration gradient, the biomass variety was considered acceptable. The proliferation of Chlorella after storage was also tested. The results showed that the Chlorella remained active after 30 days of storage, with no significant increase in biomass (Fig. 1H). Given the results above, Chlorella as a cell-based therapy might weaken the common limitation of poor storage stability and high storage cost. Moreover, the

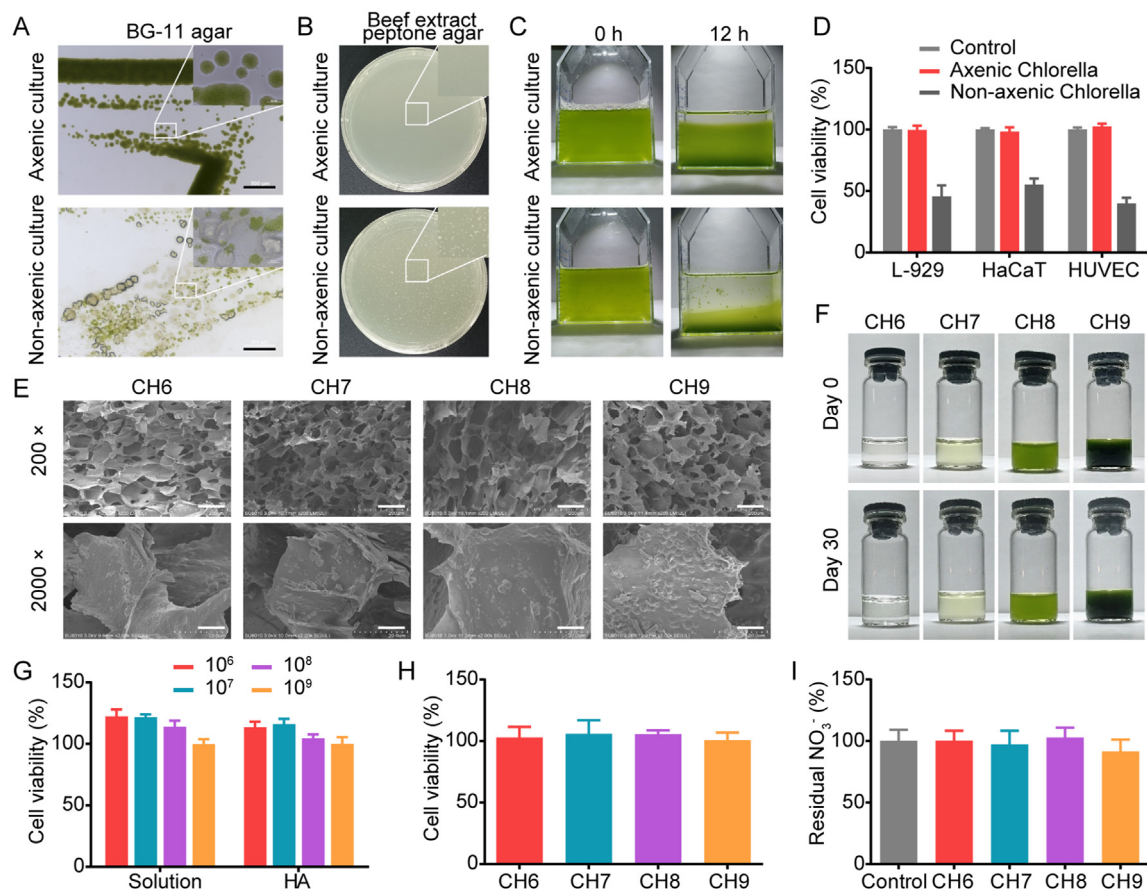


**Figure 1** Chlorella axenic culture and characterization of Chlorella hydrogels. (A) Axenic validation of Chlorella with BG-11 agar plate detected by an inverted fluorescence microscope. Scale bars: 500  $\mu$ m. (B) Axenic validation of Chlorella with beef extract peptone agar plates detected by colony count. (C) Re-suspending stability of Chlorella in BG-11 medium for 12 h standing, 37  $^{\circ}$ C, 800 lx. (D) Cytotoxicity of Chlorella ( $1 \times 10^9$  cell/mL) on L-929, HaCaT and HUVEC cells for 24 h ( $n = 6$ ). (E) SEM photographs of Chlorella hydrogels. Scale bars: 100  $\mu$ m in 200  $\times$ , 10  $\mu$ m in 2000  $\times$ . (F) Photographs of Chlorella hydrogels after preparation and Day 30 after storage. (G) Proliferation of axenic Chlorella in BG-11 medium and the hydrogels with BG-11 for 24 h, 37  $^{\circ}$ C, 800 lx, respectively ( $n = 6$ ). The concentrations of axenic Chlorella:  $1 \times 10^6$ ,  $1 \times 10^7$ ,  $1 \times 10^8$  and  $1 \times 10^9$  cell/mL. (H) Proliferation of axenic Chlorella in the hydrogels after storage for 30 days, 4  $^{\circ}$ C, dark ( $n = 6$ ). (I) Residual NO<sub>3</sub><sup>-</sup> in axenic Chlorella hydrogels after storage for 30 days, 4  $^{\circ}$ C, dark ( $n = 6$ ). Data are presented as mean  $\pm$  SD.

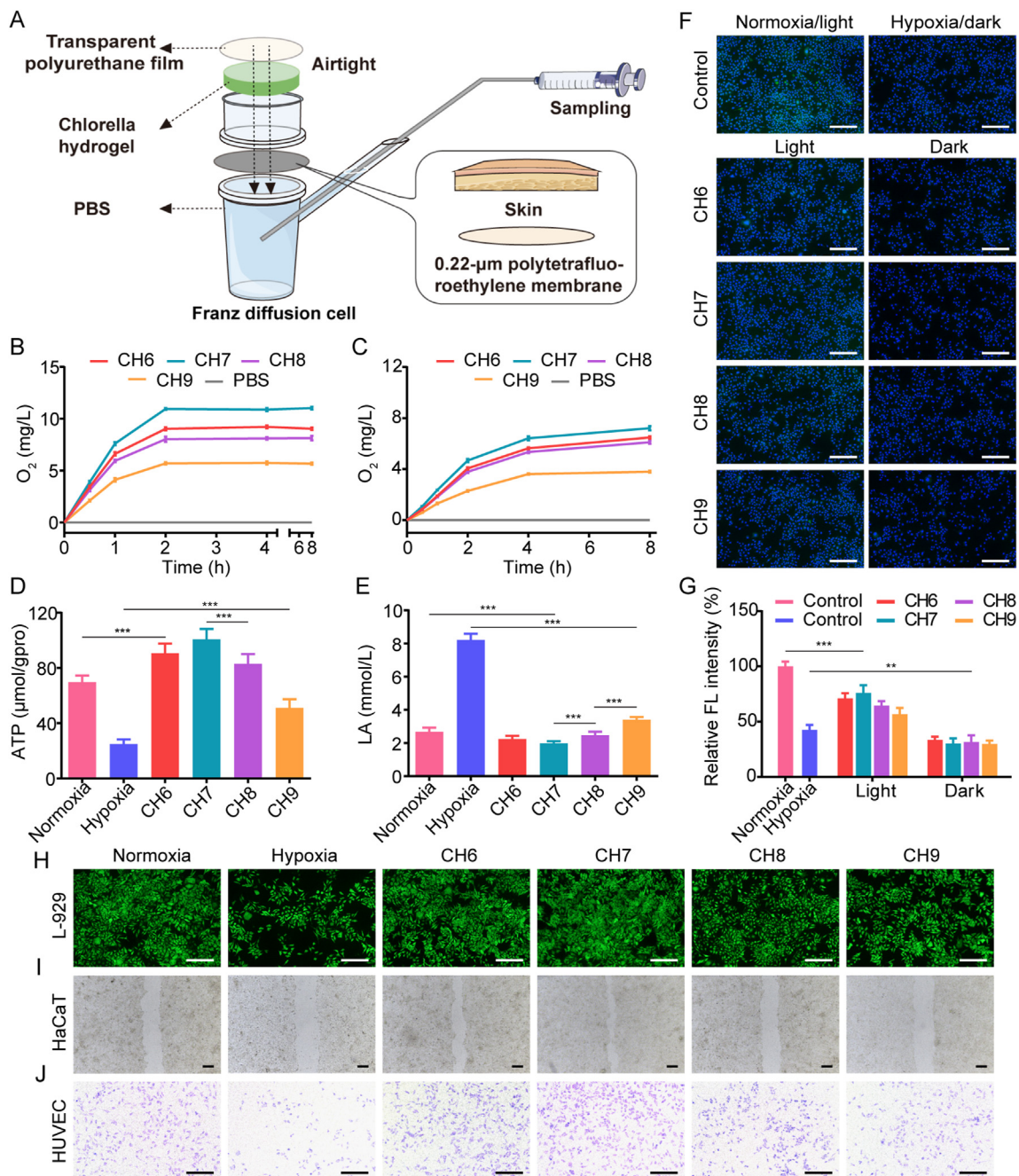
concentrations of NO<sub>3</sub><sup>-</sup> were detected after storage (NO<sub>3</sub><sup>-</sup> is the main constituent of the BG-11 medium). The results indicated that NO<sub>3</sub><sup>-</sup> was not completely metabolized (Fig. 1I). In addition to supplying nitrogen for Chlorella heterotrophy, the remaining NO<sub>3</sub><sup>-</sup> could also be converted into NO<sub>2</sub><sup>-</sup> by the xanthine oxidase in the wound tissue, further providing NO for angiogenesis<sup>34,35</sup>.

### 3.3. *In vitro* oxygen production by Chlorella

Franz diffusion cell covered with an airtight transparent polyurethane film was employed to measure the dissolved oxygen produced by Chlorella hydrogels (Fig. 2A). Continuous low-intensity illumination (800 lx, with daily used LED light) was selected, which was close to the average intensity in the daylighting room. The results showed that oxygen in the receptor cells of CH6, CH7 and CH8 groups was all supersaturated after 2 h incubation (Fig. 2B), indicating the superior oxygen production ability. Among them, CH7 made the highest oxygen level, up to 11.0 mg/L. The peak concentration and the peak time of oxygen were not good as that with the illumination commonly used (short light time with high density)<sup>22,36,37</sup>, but the oxygen level could be

maintained longer. As the tissue remodeled, fluid exchange through the wound gap was inhibited, while oxygen permeating through the re-generated skin gradually played an important role (Supporting Information Fig. S3). Therefore, the transdermal efficiency of oxygen was investigated. As shown in Fig. 2C, although the oxygen permeation was inhibited by skin, the oxygen level in all the groups with Chlorella was enhanced. The results demonstrated that the Chlorella could effectively supply oxygen during the whole therapeutic period. In all the results above, the oxygen production efficacy first increased and then decreased as the concentration of Chlorella enhanced (Fig. 2B and C). The decrease in CH8 and CH9 groups was due to the respiration of Chlorella and the reduced illumination intensity in the lower layer (Supporting Information Fig. S4). Similarly, Chlorella-respiration might also worsen the hypoxia without illumination *in vivo*.

Then, the effect of produced oxygen on breathing pattern inversion was evaluated *in vitro*. The results showed that ATP level was enhanced and the LA content was reduced in L-929 cells treated with Chlorella hydrogels (Fig. 2D and E), reflecting a shift in the breathing pattern to aerobic respiration. CH6, CH7 and CH8 groups even performed better than the normoxia group. This was



because the oxygen level in the pre-deoxygenated medium could be restored more rapidly by dissolved oxygen than the gaseous one. Oxygen-based treatments, such as hyperbaric oxygen therapy, commonly induced system oxygen toxicity<sup>16</sup>. In our study, the undesirable intracellular ROS following oxygen recovery was assessed by DCFH-DA. Although the intracellular ROS in groups with Chlorella was increased under light, it was significantly lower

than that of the normoxia group (Fig. 2F and G), showing excellent biocompatibility. The low toxicity might be due to the depletion of ROS by Chlorella (verified below). The above results confirmed that the axenic Chlorella could effectively improve hypoxia and diminish the side effects of oxygen toxicity.

Tissue regeneration is a synergy process. Fibroblasts are the main component of the dermis and can benefit other cells through

paracrine. The re-epithelialization is a typical indicator of wound healing and is widely mimicked by scratch wound healing of keratinocytes<sup>38</sup>. Endothelial cells are essential in vascularization to ameliorate ischemia<sup>39</sup>. The vascularization is reflected by the Transwell migration of endothelial cells<sup>22</sup>. The *in vitro* remission on wound tissue was characterized with L-929, HaCaT and HUVEC cells. The results showed that Chlorella hydrogels could effectively promote the proliferation of L-929 cells, the migration of HaCaT cells and the Transwell migration of HUVEC cells by oxygen production (Fig. 2H–J and Supporting Information Fig. S5).

### 3.4. *In vitro* glucose consumption by Chlorella

The effect of living Chlorella on glucose consumption was assessed *in vitro*. As shown in Fig. 3A, Chlorella consumed glucose in a concentration-dependent manner. The rapid consumption might benefit from its excellent metabolic activity. Chlorella with a concentration of  $1 \times 10^9$  cell/mL could completely consume 33 mmol/L glucose within 12 h under 800 lx continuous light. Compared with the dark condition, the glucose consumption significantly improved with illumination (Fig. 3A), which was due to the light-activated bioactivity of Chlorella<sup>40</sup>. The light condition with short illumination time and high intensity was also investigated (10,000 lx, 1 h:11 h light/dark). The glucose concentration was slightly reduced compared with that in the dark, but not so good as that in the 800 lx group (Fig. 3A). The results suggest that the consumption efficacy was mainly affected by illumination time that could keep the Chlorella active, rather than light intensity. Most of the light conditions in algae-related therapeutics were set for optimizing oxygen production, while the function of glucose consumption was ignored. Then, whether nitrogen supplements (recognized nutrients for algae) competitively inhibited the utilization of glucose was evaluated. The outcomes were approximate in the BG-11 medium and the normal saline (Supporting Information Fig. S6), illustrating that the BG-11 medium as an N source did not affect the glucose consumption by Chlorella.

The consumption pathway of glucose was further verified. After 12 h incubation, the Chlorella was inactivated, and the glucose inside the Chlorella was measured. Except 3.4–3.7 mmol/L glucose was detected in  $1 \times 10^9$  cell/mL Chlorella groups, there was nearly no glucose in other groups (Fig. 3B). The detected glucose was considered to be intrinsic to Chlorella (Supporting Information Fig. S7). These results indicate that the glucose in the exogenous medium was consumed by the Chlorella through the metabolic pathway rather than the adsorption route, and it might be solidified into nutrients such as polysaccharides, fat and protein<sup>25</sup>.

Then, the glucose consumption of Chlorella hydrogels was measured with Transwell, mimicking the wound tissue. The glucose consumption was also concentration-dependent (Fig. 3C). CH8 and CH9 groups performed well with 800 lx illumination, and the glucose concentrations in the lower chamber were decreased by 5.8 and 12.9 mmol/L within 12 h, respectively. Since the glucose concentration in wound tissue was 3–5 mmol/L<sup>41</sup>, it was suggested that the glucose could be effectively consumed by Chlorella with relatively high biomass under the light.

The cell viability of cell-based therapeutics was commonly reduced by the high-glucose microenvironment<sup>42</sup>. However, living Chlorella, as a natural glucose processing plant, was unaffected.

### 3.5. *In vitro* ROS depletion by Chlorella

The depletion of ROS ( $\text{H}_2\text{O}_2$ ,  $\cdot\text{OH}^-$  and  $\cdot\text{O}_2^-$ ) by living Chlorella was evaluated with a BG-11 medium. ROS depletion rate was enhanced as the concentration of Chlorella increased (Fig. 3D–F). Chlorella with a concentration of  $1 \times 10^8$  and  $1 \times 10^9$  cell/mL could rapidly deplete  $\text{H}_2\text{O}_2$  and inhibit the generation of  $\cdot\text{OH}^-$ . Moreover, the production of  $\cdot\text{O}_2^-$  was also reduced in the  $1 \times 10^9$  cell/mL group. Notably, the ROS depletion was considered unaffected by light, unlike the glucose consumption. This was because the high-level internal antioxidants (such as lutein and carotene<sup>26</sup>) could straightforwardly neutralize ROS by oxidation–reduction reactions. Then, Transwell was employed for further evaluation. The results demonstrated similar trends to that of the Chlorella solution (Supporting Information Fig. S8).

The advantages of ROS depletion for tissue regeneration were also assessed *in vitro*. All the groups with Chlorella could significantly restore the proliferation of L-929, ameliorate the HaCaTs scratch healing and enhance the HUVEC Transwell migration (Fig. 3G–I and Supporting Information Fig. S9).

### 3.6. *In vitro* nutrition supplement by inactivated-Chlorella (Chlorella contents)

Chlorine dioxide is widely used for water purification and is considered non-toxic to the human body with suitable concentration<sup>43</sup>. In this study, chlorine dioxide was employed to inactivate Chlorella *in situ*. The efficiency and toxicity of the inactivation were exemplified with CH8. Hydrogels in white represented that the Chlorella was inactivated, and the green part represented the active one (Fig. 4A and Supporting Information Fig. S10). 5 ppm chlorine dioxide could effectively kill the Chlorella, and the process was nearly suspended after 15 min, as 76.7% at 15 min and 83.1% at 12 h (Fig. 4B). Since excessive chlorine dioxide is cytotoxic, the concentration of chlorine dioxide passed through the hydrogels was measured. The results show that the peak residual chlorine dioxide concentration in the lower chamber of the 5 ppm group was less than 0.01 ppm and had no cytotoxicity (Fig. 4C and D). This might be because the chlorine dioxide was buffed by hydrogels and depleted during the inactivation. It is worth mentioning that Chlorella axenic culture is necessary to avoid the septic shock which may be caused by the massive endotoxins released from the chlorine dioxide-inactivated Chlorella-associated bacteria<sup>44</sup>.

The permeability of the Chlorella cell membrane was increased after inactivation, accelerating the release of the contents. The diffused Chlorella contents were representatively quantified, including carbohydrate, protein and nucleic acid. After 12 h incubation, about 18.8% carbohydrate, 11.3% protein and 7.7% nucleic acid were released from the hydrogels with 5 ppm chlorine dioxide (Fig. 4E). Then, the nutrition supplement capacity of inactivated-Chlorella was assessed *in vitro* with the basic cell culture medium. As shown in Fig. 4F and Supporting Information Fig. S11, the proliferation of L-929 cells was significantly enhanced in CH8-C and CH9-C groups. The migration of HaCaT and Transwell migration of HUVEC were also improved (Fig. 4G and H, and Fig. S11). Given the rapid inactivation rate, wound tissues only need to keep static within 15–20 min to utilize the Chlorella contents as a nutrition supplement without toxicity.

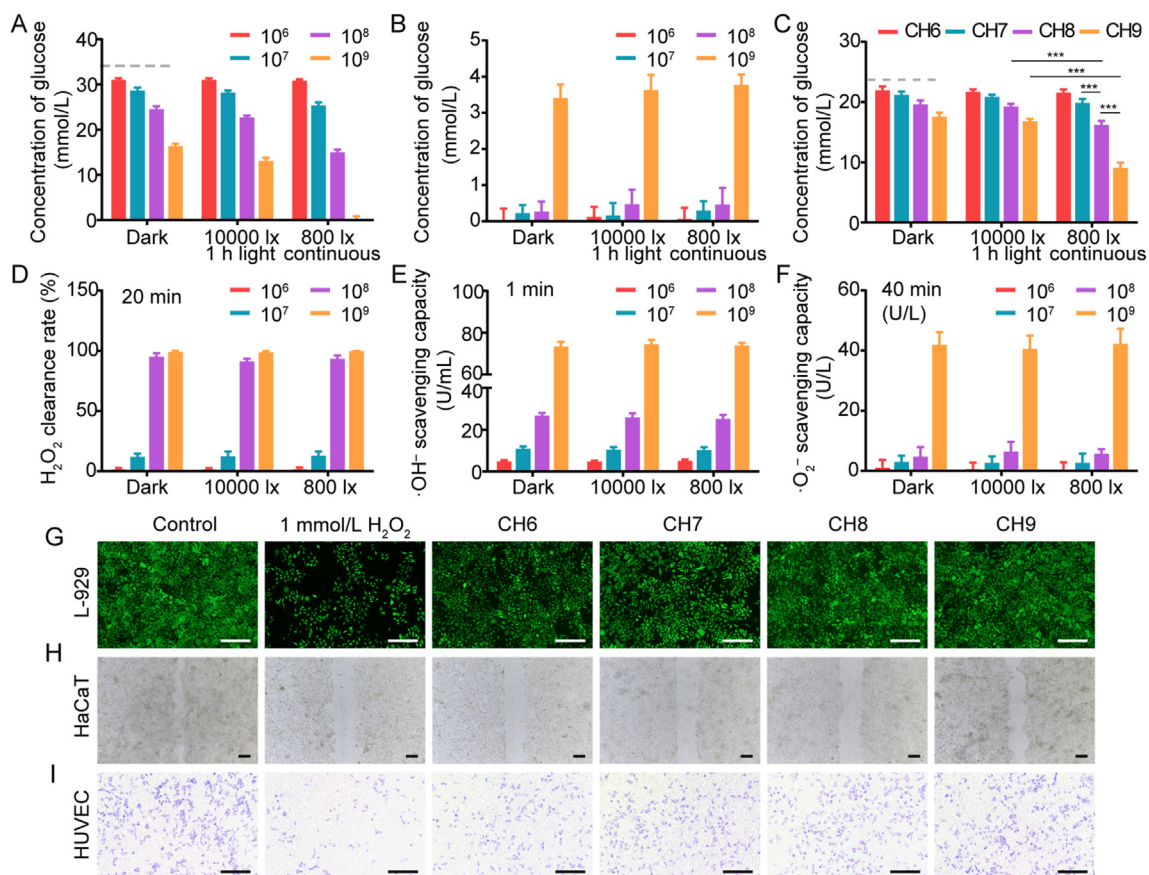


**Figure 3** Glucose and ROS depletion by Chlorella. (A) Glucose remaining in the BG-11 medium (with 33 mmol/L glucose) after 12 h incubation with Chlorella. The concentrations of Chlorella in the medium were selected as  $1 \times 10^6$ ,  $1 \times 10^7$ ,  $1 \times 10^8$  and  $1 \times 10^9$  cell/mL ( $n = 6$ ). (B) Glucose inside the Chlorella after 12 h incubation ( $n = 6$ ). (C) Glucose remaining in the lower chamber of the transwell after 12 h incubation with Chlorella hydrogels ( $n = 6$ ). A–C: 37 °C, dark/10,000 lx (1 h:11 h light/dark)/continuous 800 lx. Dotted lines marked the glucose concentration remaining in the control group. (D–F) The depletion of H<sub>2</sub>O<sub>2</sub> and the inhibition of ·OH<sup>-</sup>/·O<sub>2</sub><sup>-</sup> generation by Chlorella in BG-11 medium, 37 °C, dark/10,000 lx/800 lx, respectively. ( $n = 6$ ). (G–I) Effect of Chlorella hydrogels on L-929 cell proliferation, HaCaT migration and transwell migration of HUVEC, 37 °C, dark, respectively. The concentration of H<sub>2</sub>O<sub>2</sub> in the cell culture medium was 1 mmol/L. Scale bar: 200 μm. Data are presented as mean ± SD; \*\*\* $P < 0.001$ , \*\* $P < 0.01$ , \* $P < 0.05$ , marked necessarily.

### 3.7. *In vitro* ROS depletion and anti-inflammation by inactivated-Chlorella

Chlorella inactivation could avoid the hypoxia deterioration caused by Chlorella-respiration in the dark and supply nutrition to the cells, while the glucose/ROS depletion bonus of living Chlorella also disappeared. Because the glucose consumption rate was significantly reduced under dark (Fig. 3A–C), the inactivation was considered a little effect on glucose metabolism. However, regardless of under the light or in the dark, living Chlorella could deplete ROS rapidly (Fig. 3D–F). Since the antioxidants inside the Chlorella could be neutralized by chlorine dioxide<sup>45</sup>, the ROS depletion efficiency might be severely affected. Fortunately, although the ROS depletion of Chlorella solution was reduced by inactivation (Supporting Information Fig. S12), the depletion rate of inactivated-Chlorella hydrogels and Chlorella hydrogels was comparable (Fig. 5A–C). The maintained ROS depletion ability might benefit from the diffusing Chlorella contents. The contents could directly deplete ROS in the lower chamber, exempting the process of ROS diffusion to the upper chamber and uptake by living Chlorella.

Chlorella and its contents could effectively deplete ROS, while it was more attractive to inhibit the production of ROS *in situ* than scavenging *ex situ*<sup>46,47</sup>. The anti-inflammatory effects were tested. As shown in Fig. 5D–F, CH8-C and CH9-C decreased the expression of IL-6 and TNF- $\alpha$  in LPS-induced RAW 264.7 cells and reduced the production of NO, indicating that the inflammation was relieved by Chlorella contents. The Transwell migration of macrophages was detected for further proof. As shown in Fig. 5G and Supporting Information Fig. S13, migrated RAW 264.7 cells on the bottom side of the Transwell membrane decreased in CH8-C and CH9-C groups. Herein, the inactivated-Chlorella was suggested to diminish the recruitment of inflammatory cells, sequentially avoiding excessive ROS. However, living Chlorella had no effect on inflammation relief in the dark (Fig. 5G and Supporting Information Figs. S13 and S14).

Oxygen production, glucose consumption and ROS depletion were considered to be beneficial for relieving inflammation<sup>14,15,30</sup>, which was exactly the Chlorella did during the daytime. However, ROS depletion was the only remaining advantage without illumination, and the oxygen-consumption by Chlorella-respiration even became a burden. The extra anti-inflammatory effect

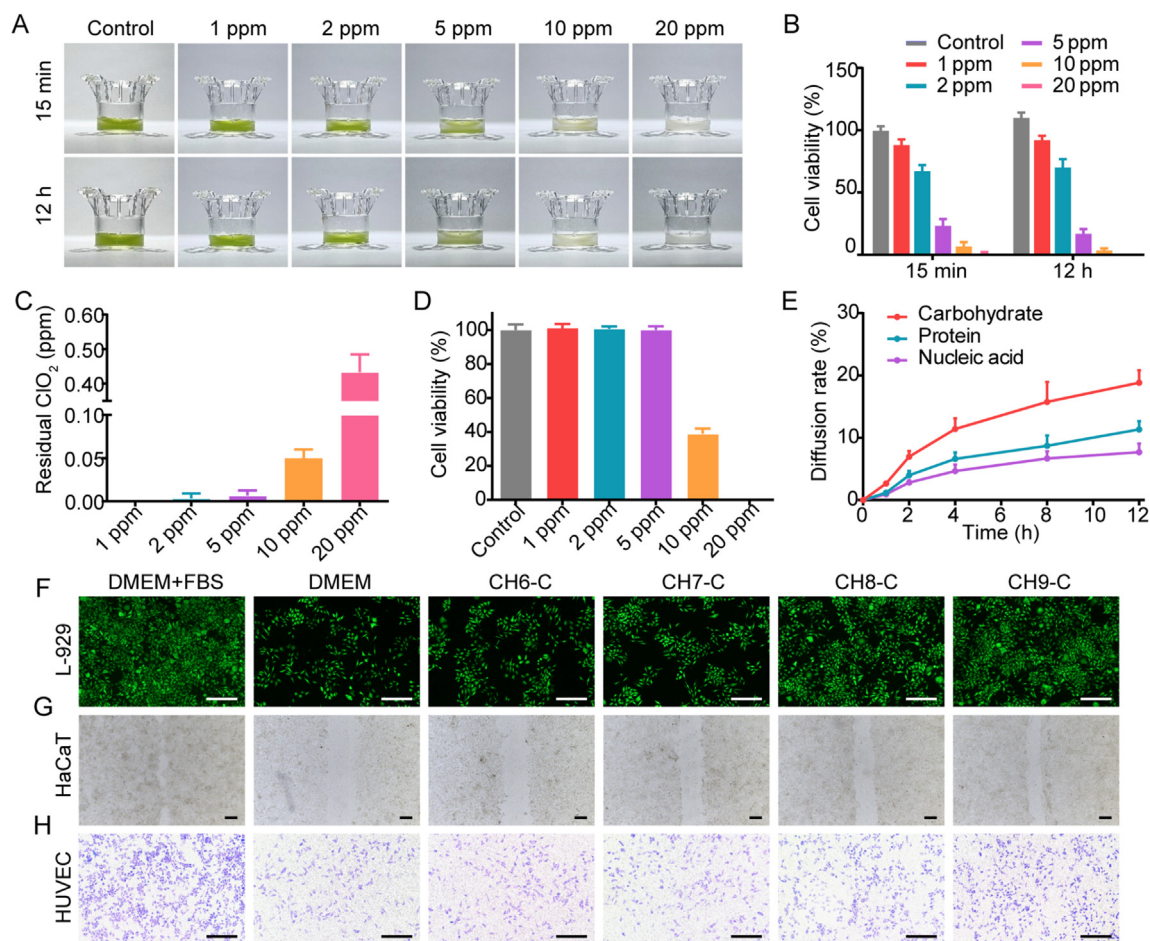


**Figure 4** Chlorella inactivation and nutrition supplement. (A) Photographs of Chlorella hydrogels inactivated by chlorine dioxide. (B) Inactivation efficiency of Chlorella by chlorine dioxide at 15 min and 12 h ( $n = 6$ ). (C) The peak concentration of residual chlorine dioxide in the lower chamber of the transwell during the inactivation ( $n = 6$ ). (D) Cytotoxicity of residual chlorine dioxide on L-929 cells ( $n = 6$ ). Cells were cultured with DMEM containing chlorine dioxide with the peak residual concentration. (E) Chlorella contents diffused from the inactivated-Chlorella hydrogels to the lower chamber of the transwell after 12 h incubation ( $n = 6$ ). (A–C, E): Chlorella concentration,  $1 \times 10^8$  cell/mL. (F–H) Effect of the inactivated-Chlorella hydrogels (Chlorella contents) on L-929 cell proliferation, HaCaT migration and transwell migration of HUVEC, 37 °C, dark, respectively. Basic DMEM was selected as the cell culture medium. Scale bar: 200  $\mu$ m. Data are presented as mean  $\pm$  SD.

provided by Chlorella inactivation was suggested to be a superior continuation of the inflammation relief during the daytime.

### 3.8. *In vivo* diabetic wound healing

Chlorella hydrogels with different biomass performed differences in oxygen production, glucose/ROS depletion and nutrition supplement. The comprehensive effects need to be further evaluated with diabetic mice. To assess the *in vivo* wound healing efficiency, an 8 mm rounded full-thickness cutaneous wound was performed. Eight groups were involved, containing non-diabetes control (control), diabetes control (DM), CH6, CH7, CH8, CH9 (12 h:12 h, 800 lx/dark for the front six groups), CH8-D (CH8, 24 h dark) and CH8-C (chlorine dioxide was added after 12 h light). The dressing was constructed as Supporting Information Fig. S15, and the hydrogels were renewed daily. The contribution of light and chlorine dioxide were respectively exemplified with  $1 \times 10^8$  cell/mL Chlorella (CH8 performed best among the selected hydrogels in the pre-experiment). As shown in Fig. 6A and B, the CH8 group gained superior performance and resembled

the control. It was considered as the cooperation of hypoxia reversal, glucose consumption as well as ROS depletion, because CH8 could continuously provide oxygen to cells for aerobic respiration (Fig. 2D and E), consume glucose to the normalized level (Fig. 3C) and rapidly deplete ROS (Fig. 3D–F and Fig. S8). CH7 and CH9 groups were also competitive in wound healing, focusing on oxygen production and glucose/ROS depletion, respectively. CH6 and CH8-D groups made limited progress. Then, the CH8 group was compared with the CH8-C group. In the CH8-C group, fewer inflammatory cells were found, and the epithelium was more regular (Fig. 6C). Furthermore, a complete stratum corneum was established when treated with CH8-C (Fig. 6C), indicating that the epithelium was normalized<sup>48</sup>. Hence, CH8-C seemed better than CH8. The optimization in the CH8-C group might be benefited from the terminated Chlorella-respiration, nutrition supplement and inflammation relief at night.

Then, granulation tissue formation and wound re-epithelialization, as typical indicators of the wound healing process, were evaluated by H&E staining (Fig. 6C and Supporting Information Fig. S16). As shown in Fig. 6D, the granulation tissue gap significantly

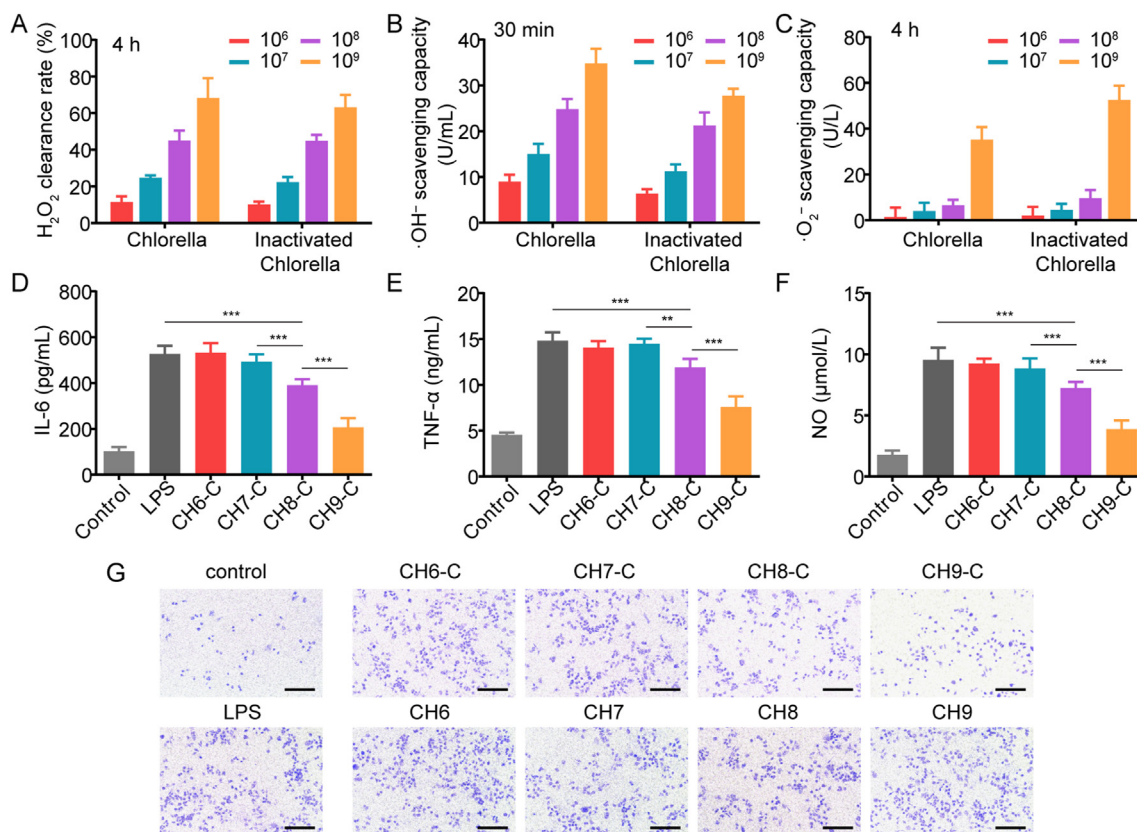


**Figure 5** ROS depletion and anti-inflammation by inactivated-Chlorella. (A–C) The comparison of hydrogels with Chlorella and inactivated-Chlorella on the depletion of H<sub>2</sub>O<sub>2</sub> and the inhibition of ·OH/·O<sub>2</sub><sup>-</sup> generation, respectively. The concentration of Chlorella was 1 × 10<sup>6</sup>, 1 × 10<sup>7</sup>, 1 × 10<sup>8</sup> and 1 × 10<sup>9</sup> cell/mL (*n* = 6). (D–F) The anti-inflammation function of hydrogels containing inactivated-Chlorella, reflected by the secretion of IL-6 and TNF-α and the production of NO in LPS-induced RAW 264.7 cells (*n* = 6). (G) Effect of inactivated-Chlorella hydrogels and Chlorella hydrogels on the transwell migration of RAW 264.7 cells. Scale bar: 200 μm. Data are presented as mean ± SD; \*\*\**P* < 0.001, \*\**P* < 0.01, \**P* < 0.05, marked necessarily.

narrowed treated with Chlorella hydrogels under light, and the result was in consistency with that of wound closure (Fig. 6B). Epithelial thickness was considered to increase during the inflammatory and proliferative stages and decrease in the remodeling stage<sup>49</sup>. The epithelium in CH8 and CH8-C groups was thinner than that of CH7 and CH9 groups and was similar to the control, indicating excellent tissue remodeling (Fig. 6E). Moreover, hair follicle density was assessed. The outcome showed that CH8 and CH8-C were also helpful in the regeneration of hair follicles, as 4.3- and 5.1-fold to the DM group, respectively (Fig. 6F). Collagen synthesis and deposition, playing crucial roles in tissue regeneration, were evaluated by Masson staining. Collagen synthesized in CH8 and CH8-C groups were approximate to the healthy skin<sup>15</sup> (Fig. 6G and H, and Fig. S15).

### 3.9. *In vivo* microenvironment regulation

Immunofluorescence staining of IL-6, Ki67, VEGF and CD31 was performed on Day 3 and Day 7, respectively. As shown in Fig. 7A and Supporting Information Fig. S17, CH8, CH9 and CH8-C groups expressed less IL-6 and were similar to the control, suggesting that the inflammatory response was relieved. On Day 3, CH7 and CH8-D groups could also reduce inflammation response compared with the DM group, while the CH6 group still struggled with the excessive inflammation. The results of Ki67 staining

showed an opposite trend (Fig. 7B and Supporting Information Fig. S18). All the groups containing Chlorella with illumination significantly increased the density of Ki67<sup>+</sup> proliferating cells on Day 7, and CH8 and CH8-C groups performed more superiorly. Then, angiogenesis was also evaluated. The results demonstrated that CH8, CH9 and CH8-C groups expressed more VEGF and CD31, indicating excellent blood vessel regeneration (Fig. 7C and D, and Supporting Information Figs. S19 and S20).

To further clarify the *in vivo* results above, microenvironments of the wound tissue were evaluated. CH6 and CH7 groups produced oxygen more effectively *in vitro* compared with CH8 and CH9 groups, while less ATP was synthesized on Day 3 (Fig. 7E). This could be explained as that excessive neutrophils and macrophages were recruited due to the high-level glucose, and the following respiratory bursts consumed most of the oxygen located in the wound tissue<sup>9</sup>, disguisedly diminishing the oxygen production efficiency. The concentration of LA was also determined, reflecting the anaerobic respiration of tissue cells and the metabolism of inflammatory cells<sup>50</sup> (Fig. 7F). Unsurprisingly, higher ATP levels and lower LA concentration were found in CH8, CH9 and CH8-C groups on Day 3, because in addition to oxygen production, hydrogels with high-biomass Chlorella could rapidly deplete glucose and ROS (Fig. 7G and H), consequently relieving the excessive inflammation (Fig. 7A). The ATP level was also responsible for tissue regeneration (Fig. 7B). Furthermore, the

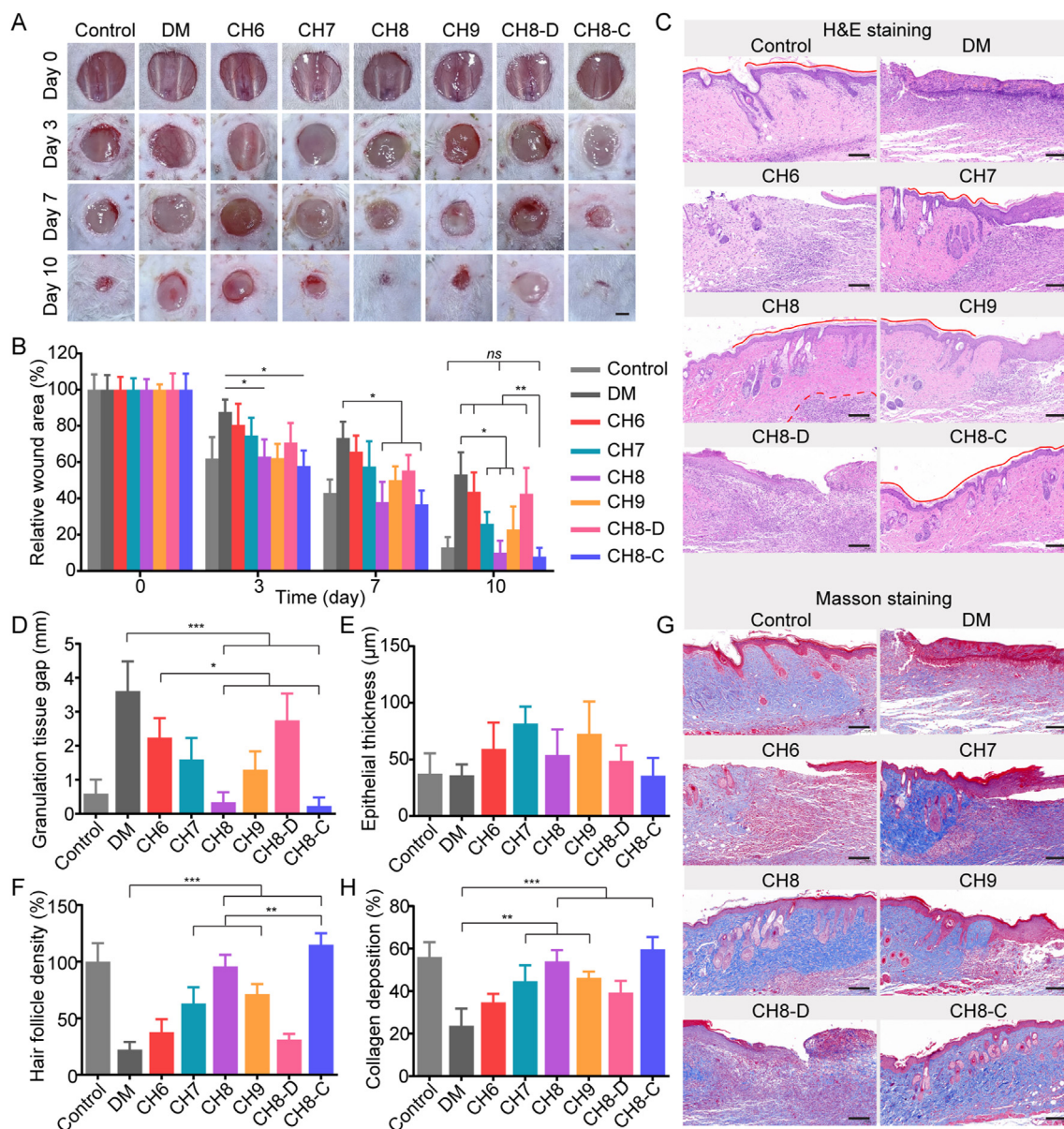


**Figure 6** *In vivo* diabetic wound healing. (A) Representative images of the diabetic wound treated with Chlorella hydrogels on Days 0, 3, 7 and 10. The scabs were removed for accurate quantification. Scale bar: 2 mm. (B) Relative wound areas of the eight groups at the pre-determined time points ( $n = 3$ ). Three mice in each group were randomly euthanized on Days 3, 7 and 10, respectively. (C) H&E staining of the wound tissue on Day 10. Red line, stratum corneum; red dotted line, the boundary of the inflammatory area. Scale bar: 50  $\mu\text{m}$ . (D–E) Quantification of granulation tissue gap and epithelial thickness of the regeneration tissue, respectively ( $n = 3$ ). (F) Quantification of hair follicle density in the middle region of the H&E staining slice ( $n = 3$ ). (G) Masson staining of the wound tissue on Day 10. (H) Quantification of collagen deposition of the wound tissue ( $n = 3$ ). Scale bar: 50  $\mu\text{m}$ . Data are presented as mean  $\pm$  SD; \*\*\* $P < 0.001$ , \*\* $P < 0.01$ , \* $P < 0.05$ , ns, not significant, marked necessarily.

glucose consumption of CH8, CH9 and CH8-C groups helped enhance the stability of hypoxia-inducible factor-1 $\alpha$  (HIF-1 $\alpha$ ), which could up-regulate the VEGF and accelerate blood vessel regeneration (Fig. 7C and D)<sup>51,52</sup>.

The *in vivo* microenvironments were also assessed on Day 7. The results show that ATP level, LA concentration and H<sub>2</sub>O<sub>2</sub> concentration in all the groups with Chlorella under illumination were significantly ameliorated compared with Day 3 (Fig. 7E, F and H), which might be due to the inflammation relief and revascularization (Fig. 7A, C and D). As the constraints of inflammation and malnutrition weakened, the therapeutic

efficiency of CH7 rebound strongly with the high-performance oxygen production. While, the superiority of CH8, CH9 and CH8-C groups was diminished, because the glucose concentration in wound tissue was also recovered with angiogenesis (Fig. 7G). Finally, the reduced pH of the wound exudate verified the tissue regeneration (Fig. 7I).

However, several issues need to be further studied before commercialization, such as the influence of Chlorella origin and culture method on the therapeutic efficiency, the long-term storage stability, and whether Chlorella can be inactivated sensitively to further improve safety and avoid secondary delivery.

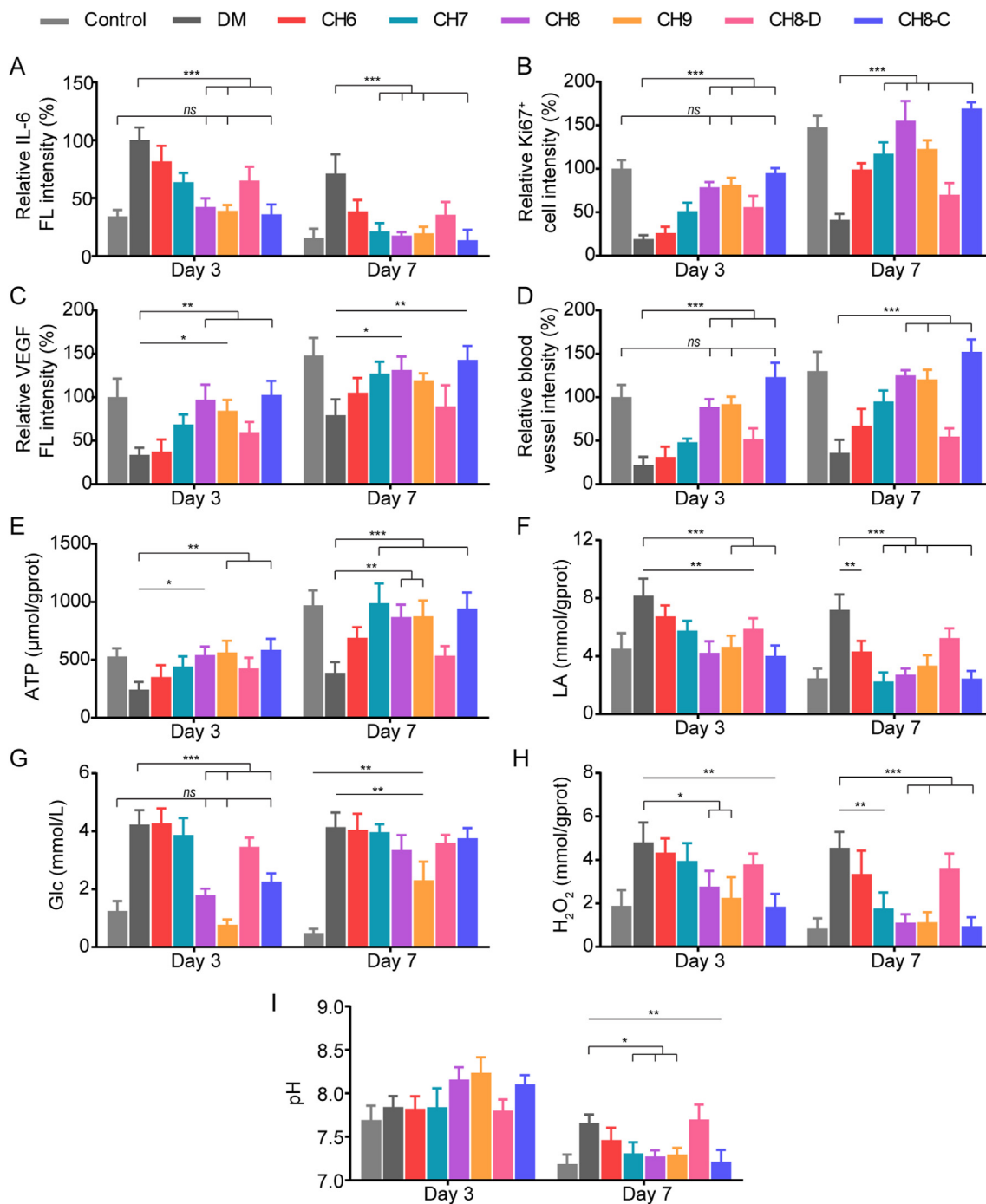


**Figure 7** Immunofluorescence staining and microenvironment regulation. (A–D) Quantitative analysis of IL-6, Ki67, VEGF and CD31 in the wound tissue on Day 3 and Day 7 after wounding ( $n = 3$ ). (E–I) ATP level, LA concentration, glucose concentration, H<sub>2</sub>O<sub>2</sub> concentration and pH of the wound tissue/exudate on Day 3 and Day 7 after wounding ( $n = 3$ ). Data are presented as mean  $\pm$  SD; \*\*\* $P < 0.001$ , \*\* $P < 0.01$ , \* $P < 0.05$ , ns, not significant, marked necessarily.

#### 4. Conclusions

In this study, the axenic culture of *Chlorella* was applied to avoid the immune response caused by associated-bacteria when it was used in wound tissue. The microenvironment regulation and therapeutic efficiency of *Chlorella* against diabetic wounds were explored *in vitro* and *in vivo*. During the daytime, living *Chlorella* was proven effective for reversing hypoxia. The high-level glucose

in the wound tissue was also reduced by *Chlorella*. At night, the *Chlorella* was inactivated *in situ* to terminate the oxygen-consumption of *Chlorella*-respiration and utilize the abundant contents for nutrition supplement and extra anti-inflammation effect. Moreover, both living and inactivated *Chlorella* was helpful in ROS depletion. All the optimizations synergistically enhanced the proliferation, migration and angiogenesis, consequently promoting the tissue regeneration. In summary, *Chlorella*

is considered to ameliorate the negative microenvironments, showing great potential for chronic diabetic wound healing.

### Acknowledgments

This work was financially supported by the National Natural Science Foundation of China (81673830), Six Talent Peaks Project in Jiangsu Province (YY053, China), Major Project and Double first-class innovative team (CPU2018GY28, China) and National Science and Technology Major Project (2017zx09101001005, China).

### Author contributions

Hangyi Wu and Pei Yang are responsible for all experiments. Hangyi Wu is responsible for the original draft preparation. Aiqin Li and Xin Jin are partly investigated in experiments. Pei Yang and Aiqin Li are responsible for statistical data analysis. Zhenhai Zhang and Huixia Lv are responsible for the experiment design, conceptualization, writing-review, validation, supervision and financial support.

### Conflicts of interest

The authors have no conflicts of interest to declare.

### Appendix A. Supporting information

Supporting data to this article can be found online at <https://doi.org/10.1016/j.apsb.2022.06.012>.

### References

- Hart T, Milner R, Cifu A. Management of a diabetic foot. *JAMA* 2017; **318**:1387–8.
- Vijayakumar V, Samal SK, Mohanty S, Nayak SK. Recent advancements in biopolymer and metal nanoparticle-based materials in diabetic wound healing management. *Int J Biol Macromol* 2019; **122**: 137–48.
- Patel S, Srivastava S, Singh MR, Singh D. Mechanistic insight into diabetic wounds: pathogenesis, molecular targets and treatment strategies to pace wound healing. *Biomed Pharmacother* 2019; **112**: 108615.
- Kunkemoeller B, Kyriakides TR. Redox signaling in diabetic wound healing regulates extracellular matrix deposition. *Antioxidants Redox Signal* 2017; **27**:823–38.
- Das A, Ghatak S, Sinha M, Chaffee S, Ahmed NS, Parinandi NL, et al. Correction of MFG-E8 resolves inflammation and promotes cutaneous wound healing in diabetes. *J Immunol* 2016; **196**:5089–100.
- Bezold V, Rosenstock P, Scheffler J, Geyer H, Horstkorte R, Bork K. Glycation of macrophages induces expression of pro-inflammatory cytokines and reduces phagocytic efficiency. *Aging (Albany NY)* 2019; **11**:5258–75.
- Loot MA, Kenter SB, Au FL, van Galen WJ, Middelkoop E, Bos JD, et al. Fibroblasts derived from chronic diabetic ulcers differ in their response to stimulation with EGF, IGF-I, bFGF and PDGF-AB compared to controls. *Eur J Cell Biol* 2002; **81**:153–60.
- Eming SA, Martin P, Tomic-Canic M. Wound repair and regeneration: mechanisms, signaling, and translation. *Sci Transl Med* 2014; **6**:265sr6.
- Lan CC, Wu CS, Huang SM, Wu IH, Chen GS. High-glucose environment enhanced oxidative stress and increased interleukin-8 secretion from keratinocytes: new insights into impaired diabetic wound healing. *Diabetes* 2013; **62**:2530–8.
- Shiekh PA, Singh A, Kumar A. Engineering bioinspired antioxidant materials promoting cardiomyocyte functionality and maturation for tissue engineering application. *ACS Appl Mater Interfaces* 2018; **10**: 3260–73.
- Nunan R, Harding KG, Martin P. Clinical challenges of chronic wounds: searching for an optimal animal model to recapitulate their complexity. *Dis Model Mech* 2014; **7**:1205–13.
- Smiell JM, Wieman TJ, Steed DL, Perry BH, Sampson AR, Schwab BH. Efficacy and safety of becaplermin (recombinant human platelet-derived growth factor-BB) in patients with nonhealing, lower extremity diabetic ulcers: a combined analysis of four randomized studies. *Wound Repair Regen* 1999; **7**:335–46.
- Wang X, Sng MK, Foo S, Chong HC, Lee WL, Tang MB, et al. Early controlled release of peroxisome proliferator-activated receptor  $\beta/\delta$  agonist GW501516 improves diabetic wound healing through redox modulation of wound microenvironment. *J Contr Release* 2015; **197**: 138–47.
- Sorci G, Riuzzi F, Giambanco I, Donato R. RAGE in tissue homeostasis, repair and regeneration. *Biochim Biophys Acta* 2013; **1833**: 101–9.
- Guan Y, Niu H, Liu Z, Dang Y, Shen J, Zayed M, et al. Sustained oxygenation accelerates diabetic wound healing by promoting epithelialization and angiogenesis and decreasing inflammation. *Sci Adv* 2021; **7**:eabj0153.
- Everett E, Mathioudakis N. Update on management of diabetic foot ulcers. *Ann N Y Acad Sci* 2018; **1411**:153–65.
- Zhao C, Wu YJ, Yang CF, Liu B, Huang YF. Hypotensive, hypoglycemic and hypolipidemic effects of bioactive compounds from microalgae and marine microorganisms. *Int J Food Sci Technol* 2015; **50**:1705–17.
- de Moraes MG, Vaz Bda S, de Moraes EG, Costa JA. Biologically active metabolites synthesized by microalgae. *BioMed Res Int* 2015; **2015**:835761.
- Khetkorn W, Rastogi RP, Incharoensakdi A, Lindblad P, Madamwar D, Pandey A, et al. Microalgal hydrogen production—a review. *Bioresour Technol* 2017; **243**:1194–206.
- Mirkovic T, Ostroumov EE, Anna JM, van Grondelle R, Govindjee, Scholes GD. Light absorption and energy transfer in the antenna complexes of photosynthetic organisms. *Chem Rev* 2017; **117**:249–93.
- Roth MS, Cokus SJ, Gallaher SD, Walter A, Lopez D, Erickson E, et al. Chromosome-level genome assembly and transcriptome of the green alga *Chromochloris zofingiensis* illuminates astaxanthin production. *Proc Natl Acad Sci U S A* 2017; **114**:E4296–305.
- Chen H, Cheng Y, Tian J, Yang P, Zhang X, Chen Y, et al. Dissolved oxygen from microalgae-gel patch promotes chronic wound healing in diabetes. *Sci Adv* 2020; **6**:eaba4311.
- Zhang W, Zhang P, Sun H, Chen M, Lu S, Li P. Effects of various organic carbon sources on the growth and biochemical composition of *Chlorella pyrenoidosa*. *Bioresour Technol* 2014; **173**:52–8.
- Li HB, Cheng KW, Wong CC, Fan KW, Chen F, Jiang Y. Evaluation of antioxidant capacity and total phenolic content of different fractions of selected microalgae. *Food Chem* 2007; **102**:771–6.
- de Jesus Raposo MF, de Moraes RM, de Moraes AM. Health applications of bioactive compounds from marine microalgae. *Life Sci* 2013; **93**:479–86.
- Montero-Lobato Z, Vázquez M, Navarro F, Fuentes JL, Bermejo E, Garbayo I, et al. Chemically-induced production of anti-inflammatory molecules in microalgae. *Mar Drugs* 2018; **16**:478.
- Zhang R, Chen J, Mao X, Qi P, Zhang X. Anti-inflammatory and anti-aging evaluation of pigment-protein complex extracted from *Chlorella pyrenoidosa*. *Mar Drugs* 2019; **17**:586.
- Shewale JG, Gelhaus HC, Ratcliff JL, Hernandez-Kapila YL. *In vitro* antiviral activity of stabilized chlorine dioxide containing oral care products. *Oral Dis* 2021. Available from: <https://doi.org/10.1111/odi.14044>.
- Xiong Y, Yan Y, Li Y. Tripterine alleviates LPS-induced inflammatory injury by up-regulation of miR-146a in HaCaT cells. *Biomed Pharmacother* 2018; **105**:798–804.
- Wang S, Zheng H, Zhou L, Cheng F, Liu Z, Zhang H, et al. Nano-enzyme-reinforced injectable hydrogel for healing diabetic wounds

- infected with multidrug resistant bacteria. *Nano Lett* 2020;**20**:5149–58.
31. Guo W, Zhu S, Feng G, Wu L, Feng Y, Guo T, et al. Microalgae aqueous extracts exert intestinal protective effects in Caco-2 cells and dextran sodium sulphate-induced mouse colitis. *Food Funct* 2020;**11**:1098–109.
  32. de Melo RG, de Andrade AF, Bezerra RP, de Araújo Viana Marques D, da Silva Jr VA, Paz ST, et al. Hydrogel-based *Chlorella vulgaris* extracts: a new topical formulation for wound healing treatment. *J Appl Phycol* 2019;**31**:3653–63.
  33. Ramirez-Acuña JM, Cardenas-Cadena SA, Marquez-Salas PA, Garza-Veloz I, Perez-Favila A, Cid-Baez MA, et al. Diabetic foot ulcers: current advances in antimicrobial therapies and emerging treatments. *Antibiotics (Basel)* 2019;**8**:193.
  34. Jones AM. Dietary nitrate supplementation and exercise performance. *Sports Med* 2014;**44**(Suppl 1):S35–45.
  35. Li H, Samouilov A, Liu X, Zweier JL. Characterization of the magnitude and kinetics of xanthine oxidase-catalyzed nitrate reduction: evaluation of its role in nitrite and nitric oxide generation in anoxic tissues. *Biochemistry* 2003;**42**:1150–9.
  36. Wang H, Guo Y, Wang C, Jiang X, Liu H, Yuan A, et al. Light-controlled oxygen production and collection for sustainable photodynamic therapy in tumor hypoxia. *Biomaterials* 2021;**269**:120621.
  37. Guo M, Wang S, Guo Q, Hou B, Yue T, Ming D, et al. NIR-responsive spatiotemporally controlled Cyanobacteria micro-nanodevice for intensity-modulated chemotherapeutics in rheumatoid arthritis. *ACS Appl Mater Interfaces* 2021;**13**:18423–31.
  38. Zheng X, Narayanan S, Sunkari VG, Eliasson S, Botusan IR, Grünler J, et al. Triggering of a Dll4–Notch1 loop impairs wound healing in diabetes. *Proc Natl Acad Sci U S A* 2019;**116**:6985–94.
  39. Liu C, Cui X, Ackermann TM, Flamini V, Chen W, Castillo AB. Osteoblast-derived paracrine factors regulate angiogenesis in response to mechanical stimulation. *Integr Biol (Camb)* 2016;**8**:785–94.
  40. Azaman SNA, Wong DCJ, Tan SW, Yusoff FM, Nagao N, Yeap SK. *De novo* transcriptome analysis of *Chlorella sorokiniana*: effect of glucose assimilation, and moderate light intensity. *Sci Rep* 2020;**10**:17331.
  41. Zhu Y, Zhang J, Song J, Yang J, Du Z, Zhao WQ, et al. A multi-functional pro-healing zwitterionic hydrogel for simultaneous optical monitoring of pH and glucose in diabetic wound treatment. *Adv Funct Mater* 2020;**30**:1905493. 1–9.
  42. Cao C, Zhang B, Li C, Huang Q, Fu X, Liu RH. Structure and *in vitro* hypoglycemic activity of a homogenous polysaccharide purified from *Sargassum pallidum*. *Food Funct* 2019;**10**:2828–38.
  43. Yu Y, Shi J, Xie B, He Y, Qin Y, Wang D, et al. Detoxification of aflatoxin B1 in corn by chlorine dioxide gas. *Food Chem* 2020;**328**:127121.
  44. de Montmollin E, Timsit JF. How antibiotics stewardship can be safely implemented in patients with septic shock?. *Semin Respir Crit Care Med* 2021;**42**:689–97.
  45. Kumar S, Park J, Kim E, Na J, Chun YS, Kwon H, et al. Oxidative stress induced by chlorine dioxide as an insecticidal factor to the Indian meal moth, *Plodia interpunctella*. *Pestic Biochem Physiol* 2015;**124**:48–59.
  46. Britland S, Ross-Smith O, Jamil H, Smith AG, Vowden K, Vowden P. The lactate conundrum in wound healing: clinical and experimental findings indicate the requirement for a rapid point-of-care diagnostic. *Biotechnol Prog* 2012;**28**:917–24.
  47. Shiekh PA, Singh A, Kumar A. Exosome laden oxygen releasing antioxidant and antibacterial cryogel wound dressing OxOBand alleviate diabetic and infectious wound healing. *Biomaterials* 2020;**249**:120020.
  48. Menon GK, Cleary GW, Lane ME. The structure and function of the stratum corneum. *Int J Pharm* 2012;**435**:3–9.
  49. Anjum F, Agabalyan NA, Sparks HD, Rosin NL, Kallos MS, Biernaskie J. Biocomposite nanofiber matrices to support ECM remodeling by human dermal progenitors and enhanced wound closure. *Sci Rep* 2017;**7**:10291.
  50. Porporato PE, Payen VL, De Saedeleer CJ, Pr eat V, Thissen JP, Feron O, et al. Lactate stimulates angiogenesis and accelerates the healing of superficial and ischemic wounds in mice. *Angiogenesis* 2012;**15**:581–92.
  51. Thangarajah H, Vial IN, Grogan RH, Yao D, Shi Y, Januszyk M, et al. HIF-1 $\alpha$  dysfunction in diabetes. *Cell Cycle* 2010;**9**:75–9.
  52. Thangarajah H, Yao D, Chang EI, Shi Y, Jazayeri L, Vial IN, et al. The molecular basis for impaired hypoxia-induced VEGF expression in diabetic tissues. *Proc Natl Acad Sci U S A* 2009;**106**:13505–10.